

Perfect Lattice Perturbation Theory: A Study of the Anharmonic Oscillator

W. Bietenholz^a and T. Struckmann^b

^a HLRZ c/o Forschungszentrum Jülich
52425 Jülich, Germany

^b Physics Department
University of Wuppertal
D-42097 Wuppertal, Germany

Preprint HLRZ 1997-67, WUB 97-35

As an application of perfect lattice perturbation theory, we construct an $O(\lambda)$ perfect lattice action for the anharmonic oscillator analytically in momentum space. In coordinate space we obtain a set of 2-spin and 4-spin couplings $\propto \lambda$, which we evaluate for various masses. These couplings never involve variables separated by more than two lattice spacings.

The $O(\lambda)$ perfect action is simulated and compared to the standard action. We discuss the improvement for the first two energy gaps ΔE_1 , ΔE_2 and for the scaling quantity $\Delta E_2/\Delta E_1$ in different regimes of the interaction parameter, and of the correlation length.

1 Introduction

The only non-perturbative access to complicated 4d quantum field theories, such as QCD, which proved successful, are Monte Carlo simulations on the lattice. They necessarily take place at a finite lattice spacing a and in a finite size L . In order to reveal information about continuum physics in an infinite volume, we have to require $a \ll \xi \ll L$, where ξ is the correlation length. In particular the finiteness of ξ/a causes serious systematic errors in practical simulations. It is now very fashionable to fight such artifacts by using “improved lattice actions” [1]. These are discretizations of the continuum action, which are supposed to display the correct scaling behavior down to a much shorter correlation length in lattice units, than it is the case for the standard lattice action.

In the literature, there are mainly two strategies to construct improved lattice actions, in particular for QCD. The first one is called Symanzik’s program [2]. One tries to eliminate the lattice spacing artifacts order by order in a – similar to the Runge and Kutta procedure for the numerical solution of ordinary differential equations. This is achieved by adding irrelevant operators. On the classical level, and in the framework of on-shell improvement [3], the standard Wilson action for QCD could be improved to $O(a)$ analytically by adding the so-called clover term [4]. On the quantum level, the coefficient of this term gets renormalized, and the quantum correction was first estimated numerically by a mean field approach [5]. The complete $O(a)$ improvement was finally determined by the ALPHA collaboration based on extensive simulations [6]. However, it seems hardly feasible to carry on this program beyond $O(a)$.

The alternative method uses renormalization group concepts to construct quasi-perfect actions. These are approximations to perfect actions, i.e. to actions which are completely free of cutoff artifacts [7]. As a fundamental difference from Symanzik’s program, this method is non-perturbative with respect to a . As a first step, this program can be realized perturbatively (in the interaction), which yields analytic expressions for the perfect quark-gluon and 3-gluon vertex functions [8, 9, 10].¹ Thus one eliminates all artifacts of $O(a^n)$ and $O(ga^n)$, such that the remaining artifacts are of $O(g^2a)$ and beyond (g is the gauge coupling). This is opposed to the action of Ref. [6],

¹Perturbatively perfect actions have also been studied for the Schwinger model, [11, 12].

which is free of artifacts in $O(g^n a)$, but plagued for instance by systematic errors in $O(a^2)$.

An extension of this program is the construction of “classically perfect actions” [13]. This approach, which is designed particularly for asymptotically free models, is non-perturbative also with respect to the coupling g . Using a multigrid procedure, one identifies the fixed point action of an renormalization group transformation. This can be done solely by minimization – the functional integral reduces to a classical field theory problem – and the fixed point action then serves as an approximatively perfect (“classically perfect”) action at finite correlation length too. In a sequence of toy models, it turned out that classically perfect actions are excellent approximations to (quantum) perfect actions, in the sense that they drastically suppress lattice spacing artifacts. The improvement achieved in this way goes far beyond first order Symanzik improvement. This has been observed for the 2d O(3) and CP(3) model [13, 14], the Schwinger model [15] and the 1d XY model [16]. In principle that program can be extended also beyond classical perfection, if one performs e.g. one real space MCRG step at finite correlation length, starting from a classically perfect action.

The construction, which is non-perturbative in a and in g , is presumably the climax of the improvement program. However, in perfect and also in classically perfect actions the couplings tend to involve infinite distances, and we can at best achieve locality in the sense of their exponential decay. For practical purposes a truncation is needed, which does some harm to the quality of the improvement. This is the main reason why the second, more sophisticated, improvement program could not be applied yet in a satisfactory way to QCD.

Here we focus on the perturbatively perfect action. It has potential applications with two respects: it can either be used directly, or as a starting point of the non-perturbative multigrid improvement [9]. A direct application of a truncated perfect quark-gluon vertex function – together with truncated perfect free quarks – to heavy quarks is presently under investigation. Preliminary results for the charmonium spectrum are given in Ref. [17].

The purpose of this paper is to test specifically such a direct application in a very simple situation. Our model is the 1d $\lambda\phi^4$ model, or anharmonic oscillator.

As a toy model, the anharmonic oscillator has a number of virtues: we

can achieve an excellent locality, such that our $O(\lambda)$ perfect action does not need any truncation of the couplings. Thus the perturbative improvement can be tested separately, without admixture of truncation effects. Moreover, our construction is based on continuum perturbation theory, and there we do not encounter any divergent loop integrals, in contrast to field theory ($d > 1$). Finally, the reduction to quantum mechanics has the advantage that the couplings we identify do not get renormalized in the full theory.

On the other hand, it is exceptionally difficult in our model to demonstrate an improvement compared to the standard action, because the latter is also very good in this case. For the harmonic oscillator it is even perfect itself, for small interaction – the regime of interest here – it is still very good, and even for moderate interactions it performs amazingly well. As a further problem we note that the performance of continuum perturbation theory, which our improvement is based on, is rather poor in this model.

The advantages and disadvantages listed above are specific for the one dimensional case.

2 The model in the continuum

The observables we are going to consider can be evaluated directly in the continuum to a fantastic accuracy. Our interest is of course not in their values, but solely in the comparison of lattice artifacts in different discretizations. We want to test the success of a specific improvement program for the lattice action.

Nevertheless we have to start by recalling some properties of the continuum system. To fix the (field theoretic) notation, we denote the Euclidean action as

$$s[\varphi] = \int dt \left[\frac{1}{2} \dot{\varphi}(t)^2 + \frac{m^2}{2} \varphi(t)^2 + \lambda \varphi(t)^4 \right]. \quad (2.1)$$

Throughout this paper we assume $m, \lambda \geq 0$, hence we only study the “symmetric phase” (as opposed to the double well). We consider the energy eigenvalues E_n , more precisely we are going to measure directly the energy gaps $\Delta E_n \doteq E_n - E_0$. An additive constant all over the spectrum is out of control, and not much of interest either. The simplest scaling quantity is

$$\frac{\Delta E_2}{\Delta E_1} \equiv \Delta E_2 \cdot \xi, \quad (2.2)$$

where ξ is the correlation length. Moreover, there is the simple relation

$$\frac{\Delta E_n(\mu^2 m^2, \mu^3 \lambda)}{\Delta E_n(m^2, \lambda)} = \mu, \quad \text{any } \mu > 0. \quad (2.3)$$

This just follows from rescaling $t \rightarrow t/\mu$ and momentum $k \rightarrow \mu k$ in the Hamiltonian (*not* rescaling all dimensional quantities). ²

The quantity (2.2) is a *scaling quantity* in the strict sense, i.e. a dimensionless ratio of physical observables. On the other hand, quantities like (2.3) may also involve unphysical normalization factors. In a field theoretic language they correspond to the *asymptotic scaling*. Actually, improved actions are designed for an improvement of scaling, but the influence on asymptotic scaling is of interest too. It has been observed before for the Gross Neveu model [20] and for pure SU(3) gauge theory [21] that “accidentally” the latter is also improved for (quasi-)perfect actions.

For $m > 0$, the strength of the interaction depends on the dimensionless parameter

$$\tilde{\lambda} \doteq \frac{\lambda}{m^3}, \quad (2.4)$$

which is obvious from eq. (2.3). The energy eigenvalues can be expanded in $\tilde{\lambda}$, but these expansions diverge at large orders (the coefficients oscillate and their absolute values grow faster than any polynomial). ³ However, a truncated series is still useful at $\tilde{\lambda} \ll 1$ (this situation is familiar from QED). ⁴ The coefficients of these expansions have been derived many times in the literature, for instance in Ref. [22],

$$\begin{aligned} \frac{\Delta E_1}{m}(\tilde{\lambda}) &\simeq 1 + 3\tilde{\lambda} - 18\tilde{\lambda}^2 + \frac{1791}{8}\tilde{\lambda}^3 - 3825\tilde{\lambda}^4, \\ \frac{\Delta E_2}{m}(\tilde{\lambda}) &\simeq 2 + 9\tilde{\lambda} - \frac{297}{4}\tilde{\lambda}^2 + \frac{9873}{8}\tilde{\lambda}^3 - \frac{1772685}{64}\tilde{\lambda}^4, \\ \frac{\Delta E_2}{\Delta E_1}(\tilde{\lambda}) &\simeq 2 + 3\tilde{\lambda} - \frac{189}{4}\tilde{\lambda}^2 + \frac{7857}{8}\tilde{\lambda}^3 - \frac{1569069}{64}\tilde{\lambda}^4. \end{aligned} \quad (2.5)$$

²This argument was made rigorous first by K. Symanzik (unpublished). The point is that the rescaling can be implemented unitarily [18].

³Note that the point $\tilde{\lambda} = 0$ is non analytic. For a discussion of large orders, see e.g. Ref. [19].

⁴We expect the same behavior also for the the couplings in the perturbatively perfect action.

Tables of explicit values at finite $\tilde{\lambda}$ are given for example in Refs. [18, 23, 24]. However, in particular for small $\tilde{\lambda}$ they can easily be reproduced from an eigenvalue problem, as described for instance in Ref. [23].

Since our construction in the following sections is also perturbative in $\tilde{\lambda}$, it is important to know how the perturbation series for the above quantities behave. Figs. 1 and 2 compare the exact function to the truncated expansion in first, second, third and fourth order.

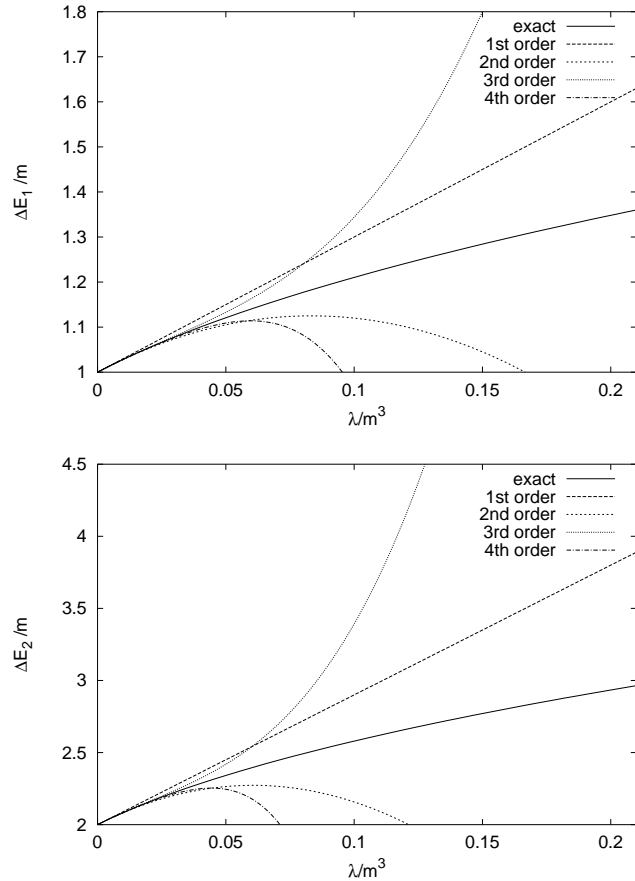


Figure 1: The ratios $\Delta E_1/m$ (on top) and $\Delta E_2/m$ (below) as functions of $\tilde{\lambda}$. The exact result is compared to the perturbation series truncated at various orders.

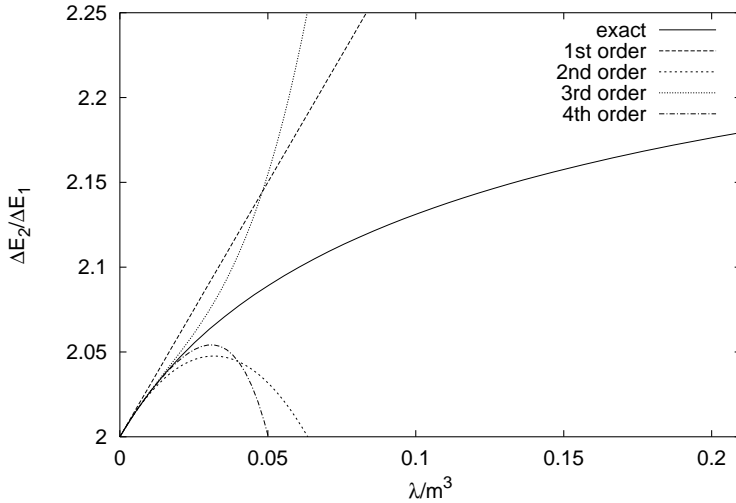


Figure 2: The ratio $\Delta E_2/\Delta E_1$ as a function of $\tilde{\lambda}$. The exact result is compared to the perturbation series truncated at various orders.

We see that the applicability of truncated expansions is restricted to very small values of $\tilde{\lambda}$. The exact range depends on the quantity considered; it agrees with the relative magnitude of the coefficients in the expansions (2.5). This range gradually expands as we proceed to higher orders.

3 The $O(\lambda)$ perfect action in momentum space

If a system is given by some lattice action, then its physical properties remain unaltered under a block variable renormalization group transformation (RGT) [7]. For suitable RGT parameters and infinite correlation length, an infinite number of iterations may lead to a finite fixed point action (FPA). A FPA is an example for a perfect action, since it is invariant under an RGT, and hence insensitive to the lattice spacing. Perfect actions also exist at any finite correlation length [7]. They reveal exact continuum scaling at any lattice spacing. For free or perturbatively interacting fields, they can be computed analytically in momentum space. This calculation simplifies if we

send the blocking factor to infinity, which amounts to a technique that we call “blocking from the continuum”. Recently this method has been applied to the Schwinger model [11] and to QCD [8]. Here we want to apply it to construct a lattice action for the anharmonic oscillator, which is perfect to $O(\tilde{\lambda})$. Our blocking uses the standard, piece-wise constant weight distribution for the original variables, and a Gaussian transformation term. For an alternative ansatz, closer to the spirit of a decimation RGT, see Ref. [25].

Our perfect lattice action $S[\phi]$ is determined by the functional integral

$$\begin{aligned} e^{-S[\phi]} &= \int D\varphi \exp\{-s[\varphi] - R[\phi, \varphi]\}, \\ R[\phi, \varphi] &= \frac{1}{2\alpha} \sum_{x \in \mathbb{Z}} \left(\phi_x - \int_{x-1/2}^{x+1/2} dt \varphi(t) \right)^2. \end{aligned} \quad (3.1)$$

Here ϕ is the lattice field, x are the lattice sites and the continuum action $s[\varphi]$ is given in eq. (2.1). The RGT parameter $\alpha > 0$ is arbitrary; for any value of α the RGT keeps the partition function invariant,

$$Z = \int D\varphi e^{-s[\varphi]} \propto \int D\phi e^{-S[\phi]}, \quad (D\phi \doteq \prod_{x \in \mathbb{Z}} \int d\phi_x), \quad (3.2)$$

and with it all expectation values. The limit $\alpha \rightarrow 0$ corresponds to the well known “ δ function RGT”.

In momentum space, this expression can be written as

$$\begin{aligned} e^{-S[\phi]} &= \int D\varphi D\sigma \exp \left\{ -\frac{1}{2\pi} \int_{-\pi}^{\pi} dk \times \right. \\ &\quad \left[\frac{1}{2} \sum_{l \in \mathbb{Z}} \varphi(-k - 2\pi l) [(k + 2\pi l)^2 + m^2] \varphi(k + 2\pi l) \right. \\ &\quad \left. + i\sigma(-k) [\phi(k) - \sum_{l \in \mathbb{Z}} \varphi(k + 2\pi l) \Pi(k + 2\pi l)] \right. \\ &\quad \left. + \frac{1}{2}\alpha \sigma(-k)\sigma(k) \right] \times \\ &\quad \left\{ 1 - \frac{\lambda}{(2\pi)^3} \int d^4 p \varphi(p_1)\varphi(p_2)\varphi(p_3)\varphi(p_4) \delta(\sum_{i=1}^4 p_i) \right. \\ &\quad \left. + O(\lambda^2) \right\}, \\ \Pi(k) &\doteq \frac{\hat{k}}{k}, \quad \hat{k} \doteq 2 \sin \frac{k}{2}, \end{aligned} \quad (3.3)$$

where we have introduced an auxiliary lattice field σ .

We denote the free continuum propagator as

$$\Delta(k) = \frac{1}{k^2 + m^2}, \quad (3.4)$$

and

$$G(k) = \sum_{l \in \mathbb{Z}} \Delta(k + 2\pi l) \Pi(k + 2\pi l)^2 + \alpha \quad (3.5)$$

is the perfect free lattice propagator, as we will see. At $m = 0$ this is the fixed point propagator, which has been calculated for free scalar theories first by Bell and Wilson, and it characterizes the FPA for the $O(N)$ model in the large N limit as well [27].

We now choose the special value $\alpha = (\sinh m - m)/m^3$, which renders the free lattice action “ultralocal” [28], i.e. it only couples nearest neighbor lattice variables,⁵

$$G(k) = \frac{\sinh m \cdot \hat{m}^2}{m^3} \frac{1}{\hat{k}^2 + \hat{m}^2}, \quad \hat{m} \doteq 2 \sinh \frac{m}{2}. \quad (3.6)$$

Our first step is the substitution

$$\tilde{\varphi}(k + 2\pi l) \doteq \varphi(k + 2\pi l) - i\sigma(k)\Delta(k + 2\pi l)\Pi(k + 2\pi l), \quad (3.7)$$

which allows us to integrate out the continuum variable $\tilde{\varphi}$. We omit the constant factor in the Gaussian integral⁶ and obtain

$$\begin{aligned} e^{-S[\phi]} &= \int D\sigma \exp \left\{ -\frac{1}{2\pi} \int_{-\pi}^{\pi} dk [i\sigma(-k)\phi(k) + \frac{1}{2}\sigma(-k)G(k)\sigma(k)] \right\} \times \\ &\quad \left\{ 1 - 3\lambda \left(\frac{1}{2m} \right)^2 \right. \\ &\quad \left. + 6\lambda \frac{1}{2m} \left[\prod_{i=1}^2 \sum_{n_i \in \mathbb{Z}} \frac{1}{2\pi} \int_{-\pi}^{\pi} dp_i \sigma(p_i)\Delta(p_i + 2\pi n_i)\Pi(p_i + 2\pi n_i) \right] \right. \\ &\quad \left. \times 2\pi\delta(p_1 + p_2)\delta_{n_1, -n_2} \right\} \end{aligned}$$

⁵This choice for the RGT parameter α also provides optimal locality in $d = 4$ [29].

⁶This is an example of an uncontrolled additive constant in $S[\phi]$, which motivates the consideration of the energy *gaps*, rather than the single eigenvalues. The same holds for the subsequent integration over $\tilde{\sigma}$, see below.

$$\begin{aligned}
& -\lambda \left[\prod_{i=1}^4 \sum_{n_i} \frac{1}{2\pi} \int_{-\pi}^{\pi} dp_i \sigma(p_i) \Delta(p_i + 2\pi n_i) \Pi(p_i + 2\pi n_i) \right] \\
& \times 2\pi \delta(\sum_{i=1}^4 [p_i + 2\pi n_i]) + O(\lambda^2) \}.
\end{aligned} \tag{3.8}$$

In a sense, this computation goes beyond the perfect QCD vertex function of Ref. [8], because it includes – for the first time in the construction of a perfect action – a loop calculation, i.e. a *quantum correction*. The continuum loop integral reads

$$\Delta(x)|_{x=0} = \frac{1}{2\pi} \int dk \Delta(k) = \frac{1}{2m} \quad (m > 0), \tag{3.9}$$

which has been inserted above. In field theory we would encounter divergences at this point, which could be regularized by some standard technique in the continuum. Here the expression is finite from the beginning, and we will see that even the limit $m \rightarrow 0$ can safely be taken at the end, when we identify the couplings in the $O(\tilde{\lambda})$ perfect lattice action.

After performing a second substitution,

$$\tilde{\sigma}(k) \doteq \sigma(k) + iG(k)^{-1}\phi(k), \tag{3.10}$$

we can integrate $\tilde{\sigma}$, and we arrive at a lattice action of the form

$$\begin{aligned}
S[\phi] = & \frac{1}{2\pi} \int_{-\pi}^{\pi} dk \frac{1}{2} \phi(-k) G(k)^{-1} \phi(k) \\
& + \lambda \left[A + \frac{1}{2\pi} \int_{-\pi}^{\pi} dk \phi(-k) B(k) \phi(k) \right. \\
& \left. + \frac{1}{(2\pi)^3} \int_{-\pi}^{\pi} d^4 p C(p) \phi(p_1) \phi(p_2) \phi(p_3) \phi(p_4) \right] + O(\lambda^2). \tag{3.11}
\end{aligned}$$

This confirms that G is the perfect free lattice propagator for the RGT chosen here. Since it differs from the standard propagator only by a constant factor and a transformation of the mass, we can also confirm the statement that for the *harmonic oscillator* the standard action is perfect already.⁷ This is very specific for the case $d = 1$ considered here.

⁷In fact, any lattice action for the harmonic oscillator is perfect [30].

The functions $B(k)$ and $C(p) = C(p_1, p_2, p_3, p_4)$ represent additional 2-variable and 4-variable couplings, while A is a constant, which is not really of interest to $O(\lambda)$.

The Wick contraction of two isolated $\tilde{\sigma}$ variables yields the lattice loop integral

$$\begin{aligned}\gamma(m) &\doteq \frac{1}{2\pi} \sum_{l \in \mathbb{Z}} \int_{-\pi}^{\pi} G(k)^{-1} \Delta(k + 2\pi l)^2 \Pi(k + 2\pi l)^2 \\ &= \frac{1}{m \cdot \sinh m \cdot \hat{m}^2} \left[2 \cosh m + e^{-m} (1 + \sinh m) - \frac{3}{m} \sinh m \right] \\ &= \frac{1}{2m} - \frac{7}{30} + \frac{11}{630} m^2 + O(m^4),\end{aligned}\tag{3.12}$$

which obeys $\gamma(m) - \gamma(-m) = 1/m$.

If we just insert this everywhere, we obtain the following $O(\lambda)$ terms,

$$\begin{aligned}A_0 &= 3 \left[\frac{1}{2m} - \gamma(m) \right]^2 \\ B_0(k) &= 3 \left[\frac{1}{m} - 2\gamma(m) \right] G(k)^{-2} \sum_{l \in \mathbb{Z}} \Delta(k + 2\pi l)^2 \Pi(k + 2\pi l)^2 \\ &= \left[\frac{1}{m} - 2\gamma(m) \right] \frac{3m^2}{2(\sinh m \cdot \hat{m}^2)^2} \times \\ &\quad \left\{ \hat{k}^4 \left(\frac{1}{2} \hat{m}^2 + \tilde{m} \right) + \hat{k}^2 \hat{m}^2 \tilde{m} + 2\hat{m}^4 \right\} \\ \text{where } \tilde{m} &\doteq 3 \left(1 - \frac{\sinh m}{m} \right) \\ C(p) &= \left[\prod_{i=1}^4 G(p_i)^{-1} \sum_{n_i \in \mathbb{Z}} \Delta(p_i + 2\pi n_i) \Pi(p_i + 2\pi n_i) \right] \times \\ &\quad \delta \left(\sum_{i=1}^4 [p_i + 2\pi n_i] \right).\end{aligned}\tag{3.13}$$

Note, however, that in the contractions in the σ^4 term, an expectation value $\langle \tilde{\sigma}(p_i) \tilde{\sigma}(p_j) \rangle$ only enforces $p_i = -p_j$ ('pairing' of the lattice momenta), while the related summation integers n_i, n_j remain independent (no 'pairing' of the continuum momenta). Therefore, such contractions yield an additional contribution $S(k)$, ($k \in [-\pi, \pi]$), which does not factorize,

$$S(k) \doteq \frac{1}{2\pi} \int_{-\pi}^{\pi} dq G(q)^{-1} \left[\sum_{n_1, n_2, n_3, n_4} \Delta(q + 2\pi n_1) \Pi(q + 2\pi n_2) \times \right.$$

$$\begin{aligned} & \Delta(-q + 2\pi n_2)\Pi(-q + 2\pi n_2)\Delta(k + 2\pi n_3)\Pi(k + 2\pi n_3) \\ & \Delta(-k + 2\pi n_4)\Pi(-k + 2\pi n_4) \Big] \delta_{\sum_i n_i, 0} (1 - \delta_{n_1, -n_2}). \end{aligned} \quad (3.14)$$

(The case $n_1 + n_2 = 0 = n_3 + n_4$ is excluded here, because it has been included before in eq. (3.13).) This modifies the constant and the bilinear term to

$$\begin{aligned} A &= A_0 + \frac{3}{2\pi} \int_{-\pi}^{\pi} dk G(k)^{-1} S(k), \\ B(k) &= B_0(k) - 6G(k)^{-2} S(k), \end{aligned} \quad (3.15)$$

while the vertex function $C(p)$, given in eq. (3.13), is not affected. It does not pick up any loop contributions, and its structure can easily be understood in the language of “building blocks” as introduced for the quark-gluon vertex [9].

The lattice spacing artifacts in the standard action can be classified in magnitudes as λa^2 , λa^4 , $\lambda a^6, \dots$, $\lambda^2 a^2, \lambda^2 a^4, \dots, \lambda^3 a^2 \dots$. In the action we have constructed now, all artifacts $\propto \lambda$ are erased. The remaining artifacts can still be $\propto a^2$, but they are multiplied at least by λ^2 . This is analogous to QCD with the perfect vertex function, where the gauge coupling g plays the rôle of λ . There the artifacts of the Wilson action start even in $O(ga)$, and the perturbative perfection pushes the leading artifact to $O(g^2 a)$.

4 The perfect couplings in coordinate space

The interaction terms involving B and C , which we derived in momentum space, turn into convolutions in coordinate space. Hence $B(r)$ describes additional 2-variable couplings (“2-spin couplings” in a solid state language) over a distance $r \in \mathbb{Z}$, and $C(r_1, r_2, r_3, 0) \doteq C(\vec{r})$ introduces 4-spin couplings,

$$\lambda \sum_{x, r \in \mathbb{Z}} B(r) \phi_x \phi_{x+r} + \lambda \sum_{x \in \mathbb{Z}, \vec{r} \in \mathbb{Z}^3} C(\vec{r}) \phi_{x+r_1} \phi_{x+r_2} \phi_{x+r_3} \phi_x.$$

We exploit lattice translational invariance, in the latter case by setting r_4 to the arbitrary value 0. $C(r_1, r_2, r_3, 0)$ is invariant under permutation of its components, and $C(\vec{r}) = C(-\vec{r})$ (but there is *no* invariance under sign flip of just one or two components of \vec{r}).

4.1 The 2-spin couplings

The function $B(k)$ is even, hence

$$B(r) \doteq B_0(r) + B_1(r) = \frac{1}{2\pi} \int_{-\pi}^{\pi} dk [B_0(k) - 6G(k)^{-2}S(k)] \cos(kr). \quad (4.1)$$

The first term, $B_0(r)$, can be computed analytically. It turns out to be the dominating contribution to $B(r)$,

$$\begin{aligned} B_0(r) &= 3 \left[\frac{1}{2m} - \gamma(m) \right] \frac{m^2}{(\sinh m \cdot \hat{m}^2)^2} \times \\ &\quad \left\{ \beta_0 \delta_{r,0} + \beta_1 [\delta_{r,1} + \delta_{r,-1}] + \beta_2 [\delta_{r,2} + \delta_{r,-2}] \right\}, \\ \beta_0 &= 2(3 + \hat{m}^2)\tilde{m} + 3\hat{m}^2 + 2\hat{m}^4, \\ \beta_1 &= -(4 + \hat{m}^2)\tilde{m} - 2\hat{m}^2, \\ \beta_2 &= \tilde{m} + \frac{1}{2}\hat{m}^2. \end{aligned} \quad (4.2)$$

(The quantities \hat{m} and \tilde{m} are defined in eqs. (3.6) and (3.13).)

Expanding in small m , we recognize the finiteness of this expression in the limit $m \rightarrow 0$,⁸

$$\begin{aligned} B_0(r) &= b_0^{(0)} \delta_{r,0} + b_1^{(0)} [\delta_{r,1} + \delta_{r,-1}] + b_2^{(0)} [\delta_{r,2} + \delta_{r,-2}], \\ b_0^{(0)} &= \frac{77}{100} - \frac{419}{1400}m^2 + O(m^4), \\ b_1^{(0)} &= \frac{91}{300} - \frac{1637}{12600}m^2 + O(m^4), \\ b_2^{(0)} &= \frac{7}{600} - \frac{31}{5040}m^2 + O(m^4). \end{aligned} \quad (4.3)$$

The additional term, $B_1(r)$, has to be evaluated numerically. It is significantly suppressed, essentially because the case $n_i = 0$, $i = 1 \dots 4$ is excluded from the summation in eq. (3.14). It typically affects the bilinear couplings only in third digit.

⁸The finiteness at $m = 0$ (“quartic oscillator”) is a very sensitive consistency test. We did not study that case – where $\tilde{\lambda} = \infty$ and $E_n = c_n \lambda^{1/3}$ – extensively, since our improved action is designed for small $\tilde{\lambda}$. However, we observed that $E_0 \propto \lambda^{1/3}$ can be fitted better for the perturbatively perfect action than for the standard action.

It turns out that also in $B_1(r)$ the couplings are restricted to distances ≤ 2 . Therefore, the entire bilinear term $B(r)$ is given by $b_i = b_i^{(0)} + b_i^{(1)}$, $i = 0, 1, 2$. These couplings are shown as functions of the mass in Fig. 3, and some precise values are given Table 1. For completeness we also include the constant A .

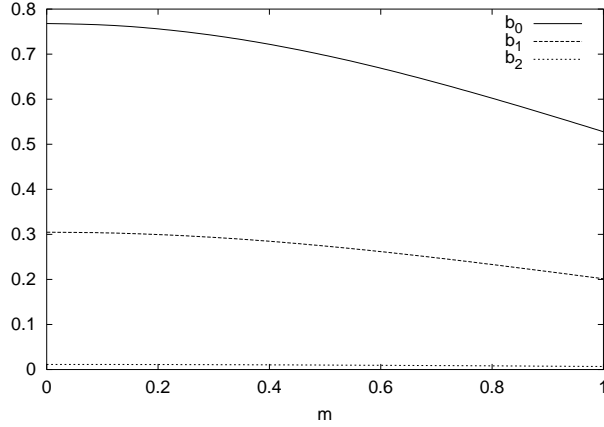


Figure 3: *The perfect bilinear couplings $\propto \tilde{\lambda}$, as functions of the mass.*

In addition we have of course the bilinear couplings of the free theory (resp. harmonic oscillator), given in eqs. (3.6) and (3.11). In coordinate space the free action reads

$$S[\phi]_{\lambda=0} = \frac{m^3}{2 \sinh m \cdot \hat{m}^2} \sum_{x,y \in \mathbb{Z}} \phi_x \left[(2 + \hat{m}^2) \delta_{x,y} - \delta_{x,y+1} - \delta_{x,y-1} \right] \phi_y . \quad (4.4)$$

4.2 The 4-spin couplings

We recall that we describe the 4-spin couplings by $C(\vec{r})$, $\vec{r} = (r_1, r_2, r_3) \in \mathbb{Z}^3$, $r_4 = 0$, that we have permutation invariance among r_1, \dots, r_4 and invariance under $\vec{r} \rightarrow -\vec{r}$, hence

$$C(\vec{r}) = \frac{1}{(2\pi)^3} \int_{-\pi}^{\pi} d^4 p \, C(p) \, \cos(\vec{p} \cdot \vec{r}) . \quad (4.5)$$

| | $m = 0$ | $m = 0.2$ | $m = 0.3$ |
|-----------|--------------|--------------|--------------|
| A | 0.1634448589 | 0.1627118789 | 0.1615030089 |
| b_0 | 0.7648784176 | 0.7560248574 | 0.7415398190 |
| b_1 | 0.3034599619 | 0.2995928547 | 0.2932745430 |
| b_2 | 0.0112505782 | 0.0110757933 | 0.0107911914 |
| C_0 | 0.2242402815 | 0.2202292735 | 0.2137198561 |
| C_1 | 0.0579948140 | 0.0568473063 | 0.0549896682 |
| C_2 | 0.0002458836 | 0.0002396038 | 0.0002295148 |
| C_{11} | 0.0386197986 | 0.0378246484 | 0.0365388182 |
| C_{12} | 0.0008364070 | 0.0008162208 | 0.0007837264 |
| C_{22} | 0.0000983088 | 0.0000956674 | 0.0000914309 |
| C_{112} | 0.0042341197 | 0.0041403776 | 0.0039890713 |

| | $m = 0.4$ | $m = 0.5$ | $m = 1$ |
|-----------|--------------|--------------|---------------|
| A | 0.1598369028 | 0.1577387270 | 0.14198250413 |
| b_0 | 0.7218143338 | 0.6973665904 | 0.52780256487 |
| b_1 | 0.2846878032 | 0.2740741694 | 0.20145092650 |
| b_2 | 0.0104063833 | 0.0099339708 | 0.00680856517 |
| C_0 | 0.2049621122 | 0.1942810514 | 0.12580113799 |
| C_1 | 0.0524997264 | 0.0494780115 | 0.03056403944 |
| C_2 | 0.0002161447 | 0.0002001630 | 0.00010708640 |
| C_{11} | 0.0348181119 | 0.0327344171 | 0.01982579170 |
| C_{12} | 0.0007405382 | 0.0006887131 | 0.00038135880 |
| C_{22} | 0.0000858306 | 0.0000791587 | 0.00004091627 |
| C_{112} | 0.0037871600 | 0.0035435707 | 0.00206185706 |

Table 1: *The $O(\lambda)$ perfect couplings for masses $0 \dots 1$.*

Note that all the singularities at $p_i = 0$ are removable, both, for finite and for vanishing mass.

It turns out that again the couplings never involve any two spins separated by a distance larger than 2. A general argument for that is given in the following subsection. This means that there are just 7 independent 4-spin couplings. We denote them as

$$\begin{aligned} C_0 &\doteq C(\vec{0}); \quad C_1 \doteq C(1, 0, 0); \quad C_2 \doteq C(2, 0, 0) \\ C_{11} &\doteq C(1, 1, 0); \quad C_{12} \doteq C(1, 2, 0); \quad C_{22} \doteq C(2, 2, 0); \quad C_{112} \doteq C(1, 1, 2). \end{aligned}$$

They all represent equivalence classes, which contain a total of 65 nontrivial couplings (keeping $r_4 = 0$ fixed). Some exact values are given in Table 1, and their mass dependence is illustrated in Fig. 4.

4.3 Locality

Assume that we calculate the perfect action to $O(\lambda^n)$ ($n \geq 1$). This involves a number of perturbative correction terms, which arise from the expectation values of the continuum field φ to some power. The highest power is $\langle \varphi^{4n} \rangle$. There, Wick contractions lead to several kinds of terms, which we classify by the power of the inverse free propagator G^{-1} . The maximal power is G^{-2n} .

For instance, in the bilinear term, which depends only on one momentum, the maximal factor is $G(k)^{-2n}$. Therefore the maximal power of \hat{k} is $\hat{k}^{4n} \propto (1 - \cos k)^{2n}$, which can be decomposed into terms $\propto \cos k, \dots, \cos 2nk$. In coordinate space this yields couplings $\propto \delta_{x,1} + \delta_{x,-1}, \dots, [\delta_{x,2n} + \delta_{x,-2n}]$.

In the terms, which couple more than two lattice variables, an analogous consideration leads to a ‘maximal’ factor $\prod_{i=1}^{2n} \cos p_i$, where the momenta p_i may be all or partially different. The observation that variables can not be coupled over distances $> 2n$ still holds.

We have seen this restriction explicitly for $n = 1$. Since the couplings are confined to such a short range, we can easily include all of them. Unlike field theory, no truncation – which does harm to the improved properties of the action – is needed. This allows us to study the quality of a perturbatively improved action separately, whereas in field theory one can only study a superposition of the improvement and the truncation scheme.

We also note that – within the limited set of couplings we deal with – locality becomes even better if the mass increases. For instance, a larger mass

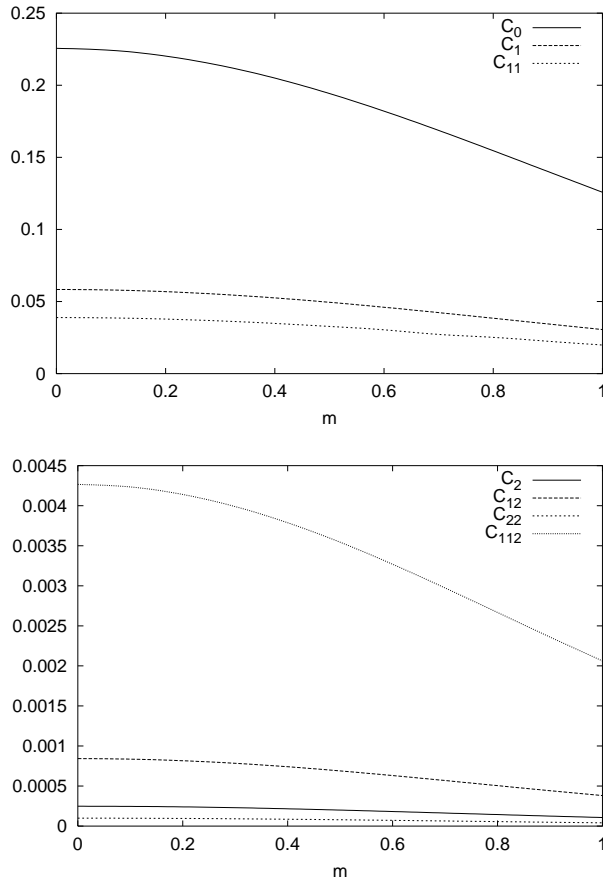


Figure 4: *The perfect 4-spin couplings $\propto \tilde{\lambda}$ as functions of m . Couplings involving distances ≤ 1 are on top, couplings involving distance 2 below.*

suppresses the couplings over distance 2 even more, relative to the leading coupling constants (see Table 1).

The restriction of the couplings to a finite range is in qualitative agreement with the effectively 1d quark-gluon vertex function (quark fields constant in all but one direction) [8]. Moreover, also the increase of locality for rising mass agrees with fermionic models and with scalar fields in higher dimensions [29].

5 Numerical results for the energy gaps

As a warming up exercise we computed the lattice partition function from direct integration. If we do so at $\tilde{\lambda} = 0$ and some $\tilde{\lambda} > 0$, we can extract an estimation for $E_0(\tilde{\lambda}) - E_0(0)$. In fact, this works much better for the perturbatively perfect action than for the standard action; for instance at $m = \lambda = 1$ the continuum ground state energy $E_{0,cont} = 0.8038$ is approximated well using the improved action, 0.8021, whereas the standard action yields 0.7111. However, this involves additive constants, which may depend on $\tilde{\lambda}$, so we focus on the energy *gaps* now.

5.1 The simulation

To compare the performance of the standard discretization and the perturbatively perfect action, we simulated both actions at correlation lengths ranging from $\xi \approx 2 \dots 5$, on a $L = 30$ lattice with periodic boundary conditions, using a standard Metropolis multi-hit algorithm. The first two energy gaps were extracted from the correlation functions $\langle 0|\phi(x)\phi(0)|0\rangle$ and $\langle 0|\phi(x)^2\phi(0)^2|0\rangle$, and the statistical errors were estimated by jackknife analysis. The decay of the ϕ^ℓ correlation function (in infinite volume) is given by⁹

$$\langle 0|\phi(x)^\ell\phi(0)^\ell|0\rangle = \sum_{n=0}^{\infty} |\langle 0|\phi^\ell|n\rangle|^2 \exp(-\Delta E_n x), \quad (5.1)$$

$(\Delta E_n \doteq E_n - E_0)$. For $\ell = 1, 2$ it reduces to¹⁰

$$\begin{aligned} \langle 0|\phi(x)\phi(0)|0\rangle &= \sum_{n=0}^{\infty} |\langle 0|\phi|2n+1\rangle|^2 \exp(-\Delta E_{2n+1}x), \\ \langle 0|\phi(x)^2\phi(0)^2|0\rangle &= \sum_{n=0}^{\infty} |\langle 0|\phi^2|2n\rangle|^2 \exp(-\Delta E_{2n}x), \end{aligned} \quad (5.2)$$

and for the harmonic oscillator we are left with

$$\begin{aligned} \langle 0|\phi(x)\phi(0)|0\rangle &= |\langle 0|\phi|1\rangle|^2 \exp(-\Delta E_1 x), \\ \langle 0|\phi(x)^2\phi(0)^2|0\rangle &= |\langle 0|\phi^2|0\rangle|^2 + |\langle 0|\phi^2|2\rangle|^2 \exp(-\Delta E_2 x). \end{aligned} \quad (5.3)$$

⁹At $L < \infty$ we actually obtain cosh functions, but we can easily measure the decay in a region, where this difference is negligible.

¹⁰Due to the mirror symmetry of the potential, eigenfunctions for E_n have parity $(-)^n$.

In our simulations we study small interaction parameters $\tilde{\lambda} \leq 0.2$. In this regime, varying the fitting ranges reveals that the $\ell = 1, 2$ correlation functions do not pick up significant contributions from energy gaps higher than the leading ones given in eq. (5.3).

5.2 Numerical results

Simulations were done for masses and anharmonic couplings in the range $m = 0.2 \dots 0.5$ and $\tilde{\lambda} = 0.001 \dots 0.2$. We compared the first two energy gaps as “asymptotic scaling quantities”, as well as $\Delta E_2/\Delta E_1$ as a scaling quantity. For a direct evaluation, we divide the lattice results by the corresponding continuum values.

Figs. 5 and 6 show the gaps $\Delta E_1(\tilde{\lambda})$ and $\Delta E_2(\tilde{\lambda})$, measured at $m = 0.5$ for the standard and perturbatively perfect action (and normalized by their corresponding continuum gaps $\Delta E_{n,cont}$). These plots show that for anharmonic couplings up to $\tilde{\lambda} \approx 0.05$ the perturbatively perfect action reproduces the continuum gaps much better than the standard action. Comparing Figs. 5, 6 with Fig. 1, one recognizes roughly the same reliability range for first order perturbation theory in the continuum. This qualitative behavior of the improvement holds for a variety of masses.

For the harmonic oscillator in infinite volume, the perfect action reproduces the continuum gaps exactly, whereas the standard action yields

$$\Delta E_{n,stan}(m) = n \cdot \text{arccosh}(1 + m^2/2). \quad (5.4)$$

(The value $\Delta E_{1,stan}(m = 0.5) \simeq 0.495$ agrees with Fig. 5). The fact that even the standard action is perfect at $\tilde{\lambda} = 0$ is reflected by the exact values of the gap ratios.

The scaling ratio $\frac{\Delta E_2}{\Delta E_1}(\tilde{\lambda})$ – again measured at $m = 0.5$ and normalized by the continuum value – is shown in Fig. 7. Unfortunately there is hardly any conclusive difference between the two types of action for that quantity.

Nevertheless, in Fig. 8, which shows the gap ratios versus $1/\xi$ at fixed $\tilde{\lambda} = 0.005$, a better performance of the perturbatively perfect action is visible at intermediate correlation length. This is a scaling plot, based on 10^9 Monte Carlo sweeps.

As we know from Fig. 2, the applicability of first order perturbation theory for $\Delta E_2/\Delta E_1$ is restricted to really tiny values of $\tilde{\lambda}$. The hope that

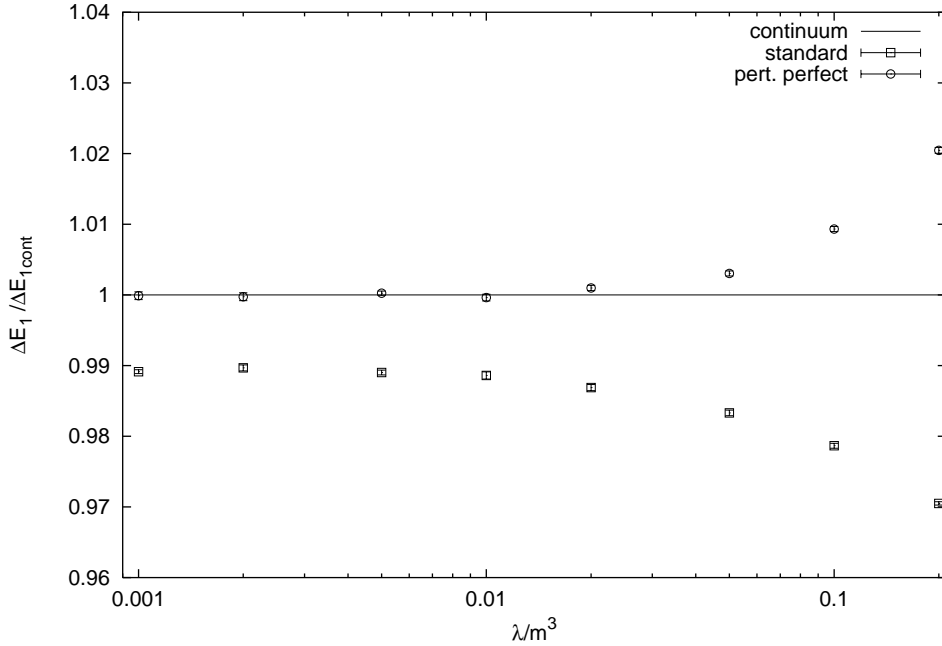


Figure 5: *The ratio $\Delta E_1/\Delta E_{1,\text{cont}}$ at $m = 0.5$, as a function of $\tilde{\lambda}$.*

the perturbatively perfect action could still perform well beyond that range can not be confirmed.¹¹ In that range itself, the improvement is extremely difficult to demonstrate, because the standard action – being perfect at $\tilde{\lambda} = 0$ – is also excellent there. The available accuracy is mainly limited by the fitting precision of the exponential decays.

6 Conclusions and outlook

We have constructed a lattice action for the anharmonic oscillator, which is perfect to first order in perturbation theory. This is the first manifestly one loop perfect lattice action¹². Comparing this action to the standard lattice

¹¹We also looked at stronger interactions, such as $\tilde{\lambda} = 0.5$, for masses $m = 0.3$ and $m = 0.5$. In that regime, the standard action scales even better than the perturbatively perfect action.

¹²For some time it was claimed that for asymptotically free theories, FPAs are not only classically perfect, but automatically also one loop quantum perfect. However, this claim

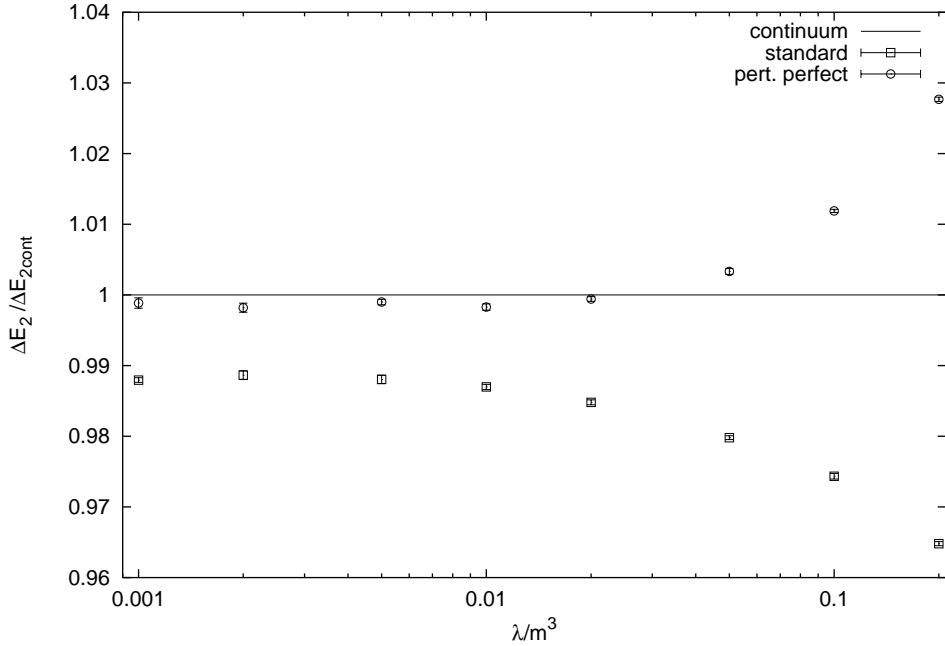


Figure 6: The ratio $\Delta E_2/\Delta E_{2,\text{cont}}$ at $m = 0.5$, as a function of $\tilde{\lambda}$.

formulation, we observe a clear improvement for the energy gaps ΔE_1 , ΔE_2 up to $\tilde{\lambda} \doteq \lambda/m^3 \sim 0.2$, over a variety of correlation lengths. As a consequence, (pseudo-)scaling laws of the type of eq. (2.3) are improved at small interactions. In field theory, this corresponds to an improved asymptotic scaling. Unfortunately, for the scaling quantity $\Delta E_2/\Delta E_1$ an improvement could only be demonstrated laboriously. It seems to be restricted to very small values of $\tilde{\lambda}$, in agreement with the performance of continuum perturbation theory. There the linear approximation is useful only for $\tilde{\lambda} \leq O(10^{-2})$. One could have hoped that the improved action is successful also beyond this regime, but it turned out that this is not the case. This can be viewed as a negative sign for the direct application of perturbatively perfect actions, but the outcome might of course depend on the model. As a further test one could simulate the perturbatively classically perfect action for the 2d O(3) model, which has been presented – but not tested – in Ref. [13] (Table 2).

has recently been disproved [30].

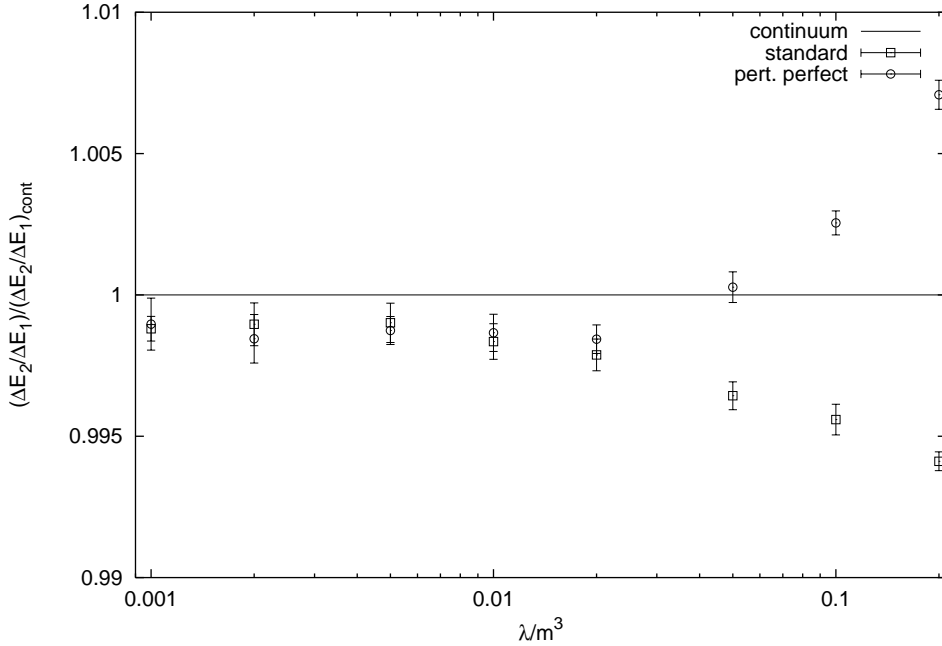


Figure 7: The ratio $\frac{\Delta E_2}{\Delta E_1} / \frac{\Delta E_2}{\Delta E_1}_{\text{cont}}$ at $m = 0.5$, as a function of $\tilde{\lambda}$.

Moreover, in the regime of tiny $\tilde{\lambda}$, the standard action is also exceptionally successful in this toy model. Therefore, an accuracy of 4 or 5 digits is required to distinguish the results of the two actions in that regime. The fit of the exponential decay does not allow for such a high precision. The behavior of other scaling quantities, like $\Delta E_3 / \Delta E_1$ etc., is even worse, i.e. the regime of successful first order perturbation theory is even smaller.¹³

Actually this construction could be carried on to $O(\tilde{\lambda}^2)$, but this includes couplings over distances 4, involving up to 8 lattice variables. Moreover, continuum perturbation theory suggests that the $O(\tilde{\lambda}^2)$ perfect action would only help to proceed to slightly larger interactions, see Fig. 2.

Still the anharmonic oscillator – and in particular the ratio of its mass gaps – may serve as a good testing ground for quasi-perfect actions, if we proceed to a *non-perturbative improvement* scheme [31]. Then one expects a

¹³As a general trend, the perturbation series gets worse if higher gaps are involved.

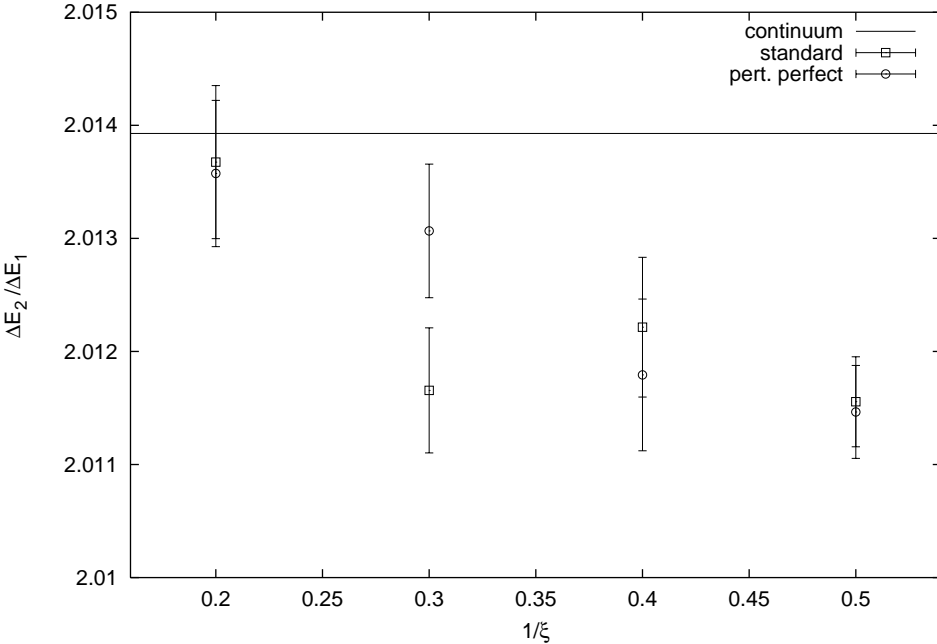


Figure 8: *The ratio $\Delta E_2/\Delta E_1$ at fixed $\tilde{\lambda} = 0.005$.*

progress also for moderate and large interactions. Thus one overcomes the disadvantages of this model listed at the end of Section 1, although some truncation of the couplings will be needed.

In particular, one may introduce an inverse temperature β in the expression for the partition function plus RGT transformation term, and send $\beta \rightarrow \infty$. Then minimization is sufficient for a multigrid inverse blocking, and in this way one can identify a *classically perfect action*. Using the standard action on the fine lattice and a fixed coarse configuration, we compared the minima for different blocking factors, and we typically observed a good convergence around blocking factor 10.¹⁴ As a test, we run the minimizer at small $\tilde{\lambda}$ and reproduced in this way the 4-spin couplings of Section 4.¹⁵

¹⁴For a finite blocking factor n one has to use the modified RGT parameter $\alpha_n = \alpha(1 - 1/n^2)$.

¹⁵Similarly, for the Schwinger model, the $O(g)$ (truncated) perfect plaquette couplings [9] could be reproduced to percent level from the classically perfect action [15] (even though a slightly different RGT was used).

The 2-spin couplings b_i arise from loop corrections, hence they are quantum effects, which are not present in the classically perfect action at small $\tilde{\lambda}$.

We can identify the classically perfect couplings over a wide range of interaction parameters. As an example, Fig. 9 compares $C_0(\tilde{\lambda})$ for the perturbatively perfect and for the classically perfect action. This figure does not imply that the perturbatively perfect approximation should be rather poor already at $\tilde{\lambda} \sim 0.1$, as we have to conclude from the simulation results.

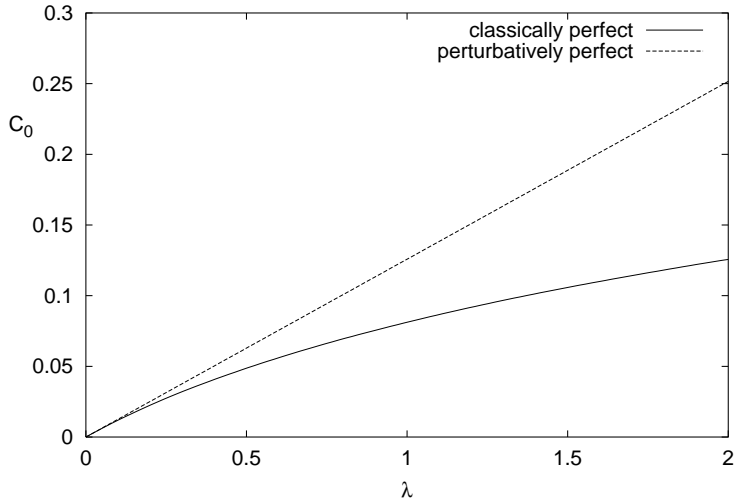


Figure 9: *The dominant 4-spin coupling C_0 at $m = 1$ as a function of the interaction parameter λ for the perturbatively perfect action and for the classically perfect action.*

Of course, the model is not asymptotically free, and the parameter λ is relevant (not just “weakly relevant”, i.e. in leading order marginal), so it does not belong to the class of models the classically perfect action is designed for. In fact, from the Table 1 we see that the bilinear contributions – that the classical approximation misses – are important. However, it might have a chance to perform well if we simulate at $\beta > 1$, where the quantum corrections to the perfect action are suppressed. The possibility that classically perfect actions work to some extent also for models, which are not

asymptotically free, is conceivable and deserves being tested.¹⁶

Finally, thanks to the simplicity of the model, one can also perform the full path integral (numerically) instead, which yields a (quantum) perfect action. As a test, we also reproduced roughly some bilinear couplings b_i from Section 4 in this way. There one is restricted to small blocking factors and lattices, such that a good convergence of the action requires iteration. Then it is interesting to compare the couplings and their performance for the classically perfect action, and the action, which is – up to numerical errors and truncation – quantum perfect. The latter is more promising, but the classically perfect action is much of interest, because in complicated field theoretic models, this is what one – maximally – has at hand.

An other important question is the convergence velocity in the multigrid procedure. In non-Abelian gauge theories, only very few iteration steps, with a small blocking factor (typically 2) are possible, hence a fast convergence to the FPA is crucial. We hope that starting from a perturbatively perfect action helps to accelerate the convergence. Also this can also be tested in the toy model discussed here.

Furthermore one can use this model to test the “cycling” procedure of shifted forward and backward blocking, proposed by the Boulder group [32]. It is tractable in higher dimensions, but not strictly based on the renormalization group. Hence a toy model analysis of the errors emerging in the “cycling” process is of interest.

At last – as we mentioned in the introduction – one may speculate that in complicated models the improvement could be pushed beyond classical perfection, by performing, say, one full block factor 2 RGT step at finite β , starting from a classically perfect action. This method can also be tested for the anharmonic oscillator.

Acknowledgment We are indebted to R. Brower, who first suggested this project. In addition we thank S. Chandrasekharan, S. Güsken, H. Hoeber, Th. Lippert, A. Okopinskaya, G. Ritzenhöfer, A. Seyfried and U.-J. Wiese for useful comments.

References

¹⁶One may also think about an extension to “semi-classical perfection”.

- [1] Proceedings of LATTICE'97, to appear in Nucl. Phys. B (Proc. Suppl.).
- [2] K. Symanzik, Nucl. Phys. B226 (1983) 187; 205.
- [3] M. Lüscher and P. Weisz, Comm. Math. Phys. 97 (1985) 59.
- [4] B. Sheikholeslami and R. Wohlert, Nucl. Phys. B259 (1985) 572.
- [5] G.P. Lepage and P. Mackenzie, Phys. Rev. D48 (1993) 2250.
 M. Alford, W. Dimm, G.P. Lepage, G. Hockney, P. Mackenzie, Phys. Lett. B361 (1995) 87.
 G.P. Lepage, Nucl. Phys. B (Proc. Suppl.) 47 (1996) 3.
- [6] M. Lüscher, S. Sint, R. Sommer and P. Weisz, Nucl. Phys. B478 (1996) 365.
 M. Lüscher, S. Sint, R. Sommer, P. Weisz and U. Wolff, Nucl. Phys. B491 (1997) 323.
- [7] K. Wilson and J. Kogut, Phys. Rep. C12 (1974) 75.
 K. Wilson, Rev. Mod. Phys. 47 (1975) 773.
- [8] W. Bietenholz and U.-J. Wiese, Nucl. Phys. B464 (1996) 319.
- [9] W. Bietenholz, R. Brower, S. Chandrasekharan and U.-J. Wiese, Nucl. Phys. B (Proc. Suppl.) 53 (1997) 921.
- [10] K. Orginos, Ph.D. Thesis, Brown University (1997).
- [11] W. Bietenholz and U.-J. Wiese, Phys. Lett. B378 (1996) 222.
- [12] F. Farchioni and V. Laliena, hep-lat/9709040.
- [13] P. Hasenfratz and F. Niedermayer, Nucl. Phys. B414 (1994) 785.
- [14] R. Burkhalter, Phys. Rev. D54 (1996) 4121.
- [15] C. Lang and T. Pany, hep-lat/9707024.
- [16] W. Bietenholz, R. Brower, S. Chandrasekharan and U.-J. Wiese, Phys. Lett. B407 (1997) 283.

- [17] K. Orginos, W. Bietenholz, R. Brower, S. Chandrasekharan and U.-J. Wiese, hep-lat/9709100, to appear in Ref. [1].
- [18] K. Banerjee, Proc. R. Soc. Lond. A364 (1978) 265.
- [19] C. Bender and T.T. Wu, Phys. Rev. D7 (1973) 1620.
- [20] W. Bietenholz, E. Focht and U.-J. Wiese, Nucl. Phys. B436 (1995) 385.
- [21] T. DeGrand, A. Hasenfratz, P. Hasenfratz and F. Niedermayer, Phys. Lett. B365 (1996) 233.
- [22] W. Caswell, Ann. Phys. (N.Y.) 123 (1979) 153.
Appendix A gives a general prescription how to compute the coefficients.
An alternative derivation is given in
A. Okopinskaya, Ann. Phys. (N.Y.) 249 (1996) 367.
- [23] S. Biswas, K. Datta, R. Saxena, P. Srivastava and V. Varma, J. Math. Phys. 14 (1973) 1190.
F. Hioe, D. MacMillen and E. Montroll, Phys. Rep. 43, No. 7 (1978) 305.
- [24] K. Banerjee, S. Bhatnagar, V. Choudhry and S. Kanwal, Proc. R. Soc. Lond. A360 (1978) 575.
B. Bacus, Y. Meurice and A. Soemadi, J. Phys. A28 (1995) L381.
- [25] M. Nauenberg, F. Kutter and M. Furman, Phys. Rev. A13 (1976) 1185.
- [26] T. Bell and K. Wilson, Phys. Rev. B11 (1975) 3431.
- [27] J. Hirsch and S. Shenker, Phys. Rev. B27 (1983) 1736.
- [28] A. Tsapalis and U.-J. Wiese, Nucl. Phys. B (Proc. Suppl.) 53 (1997) 948.
- [29] W. Bietenholz, hep-lat/9709117, to appear in Ref. [1].
- [30] P. Hasenfratz and F. Niedermayer, hep-lat/9706002.
- [31] W. Bietenholz and T. Struckmann, in preparation.
- [32] T. DeGrand, A. Hasenfratz and T. Kovács, hep-lat/9705009.